

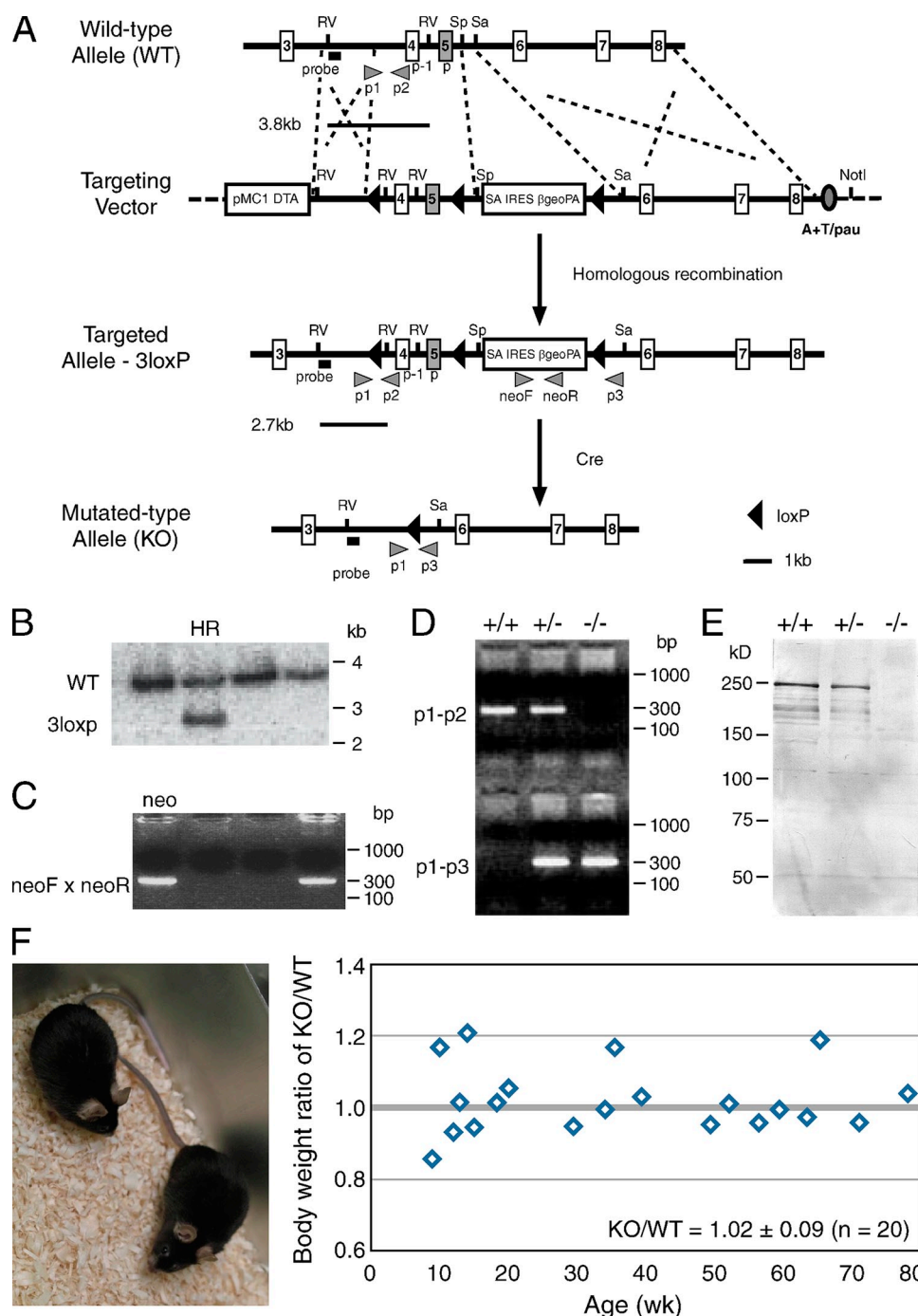
Kanai et al., <http://www.jcb.org/cgi/content/full/jcb.201309066/DC1>

Figure S1. **Targeted disruption of the mouse *kif13b* gene.** (A) Schematic drawing of the targeting strategy for the *kif13b* gene. A 2.3-kb region (exons 4 and 5, corresponding to aa 102–152) spanning the ATP-binding motif (P-loop) in the WT allele was deleted to obtain the KO allele. pMC1, promoter for DTA; DTA, diphtheria toxin; SA, splice acceptor; IRES, internal ribosome entry site; A+T/pau, AT-rich pausing signal; PA, polyA signal; p, P-loop containing exon 5; p-1, exon 4; 3–8, exons 3–8; RV, EcoRV; Sp, Spel; Sa, Sall; p1, p2, p3, primers for PCR genotyping. (B) Southern blot analyses to identify the homologous recombinant embryonic stem (ES) cell clones. Genomic DNA from ES cells was digested with EcoRV and subjected to hybridization with the “probe” indicated in A. The WT allele and targeted allele with three loxP are 3.8 kb and 2.7 kb, respectively. HR, homologous recombination. (C) PCR genotyping of the neo gene in chimeric mice using the primer set of neoF–neoR. (D) PCR genotyping of the *kif13b* gene. PCR amplifications were performed using the primer sets p1–p2 and p1–p3 to detect the WT and KO alleles, respectively. +/+, WT; +/-, heterozygote; -/-, homozygote. (E) Immunoblotting analyses of KIF13B using crude liver extracts (20  $\mu$ g protein/lane). (F, left) Photograph showing 40-wk-old WT (left) and KO (right) mice. (F, right) There are no apparent changes in body weight between WT and KO mice. The ratios of the body weight of KO to WT mice from different ages are shown (KO/WT = 1.02  $\pm$  0.09, mean  $\pm$  SD, n = 20). Each ratio was obtained from a pair of littermate male mice.



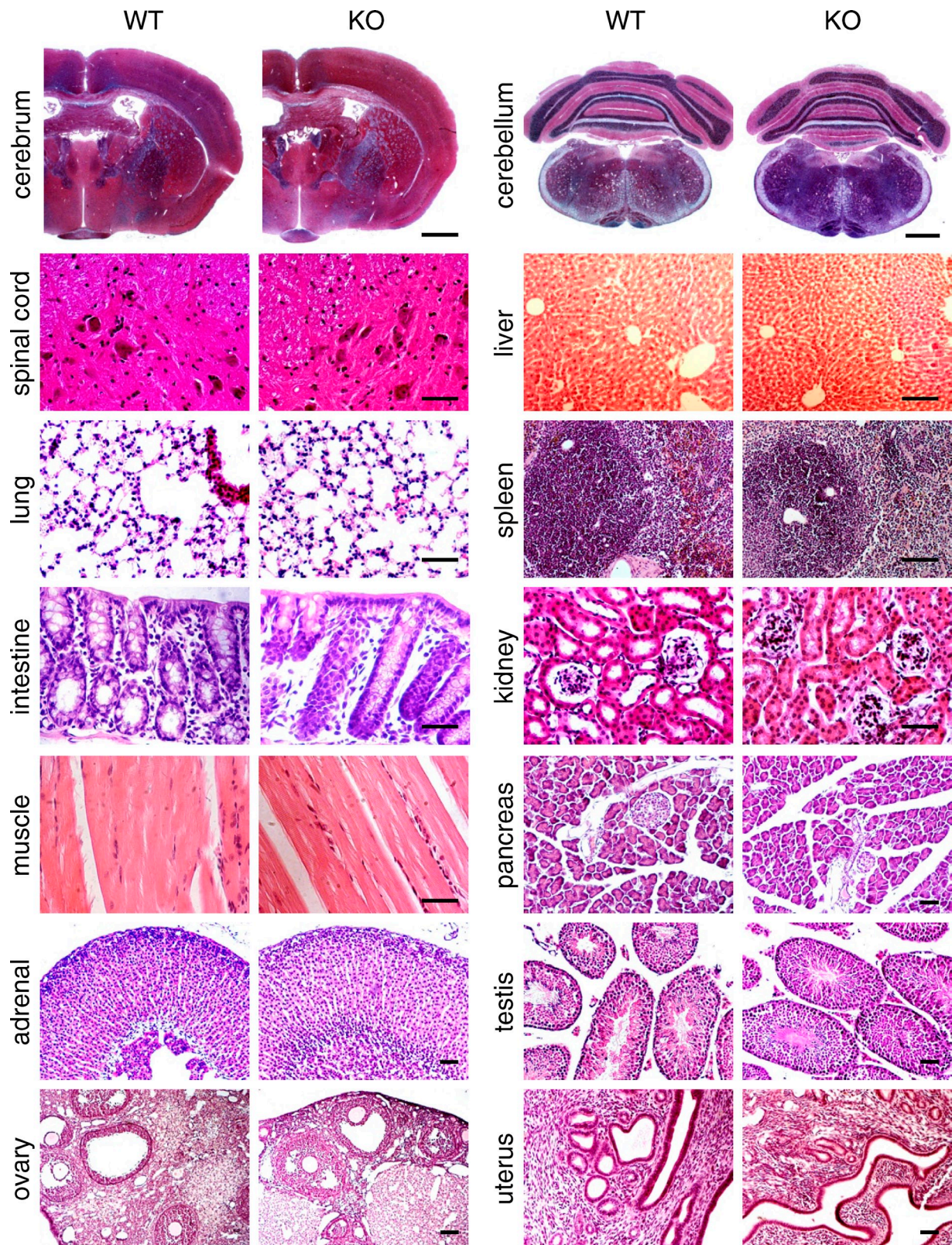


Figure S2. **Knockout mice do not show apparent histological changes.** Bodian staining (cerebrum and cerebellum) and hematoxylin/eosin staining (spinal cord, liver, lung, spleen, intestine, kidney, muscle, pancreas, adrenal, testis, ovary, and uterus) of sections from 32-wk-old WT and KO mice. No apparent changes were observed in these tissues. Bars: (cerebrum and cerebellum) 1 mm; (others) 50  $\mu$ m.

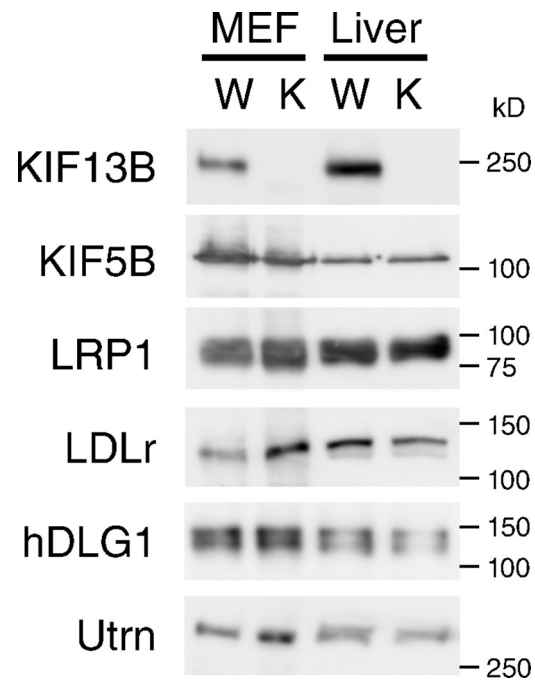


Figure S3. **Expression of KIF13B, KIF5B, LRP1, LDLr, hDLG1, and utrophin in MEFs and the liver.** Immunoblotting analyses of WT and KO MEFs and livers using antibodies against KIF13B, KIF5B, LRP1, LDLr, hDLG1, and utrophin (Utrn). Crude extracts (10 µg protein) were loaded in each lane.

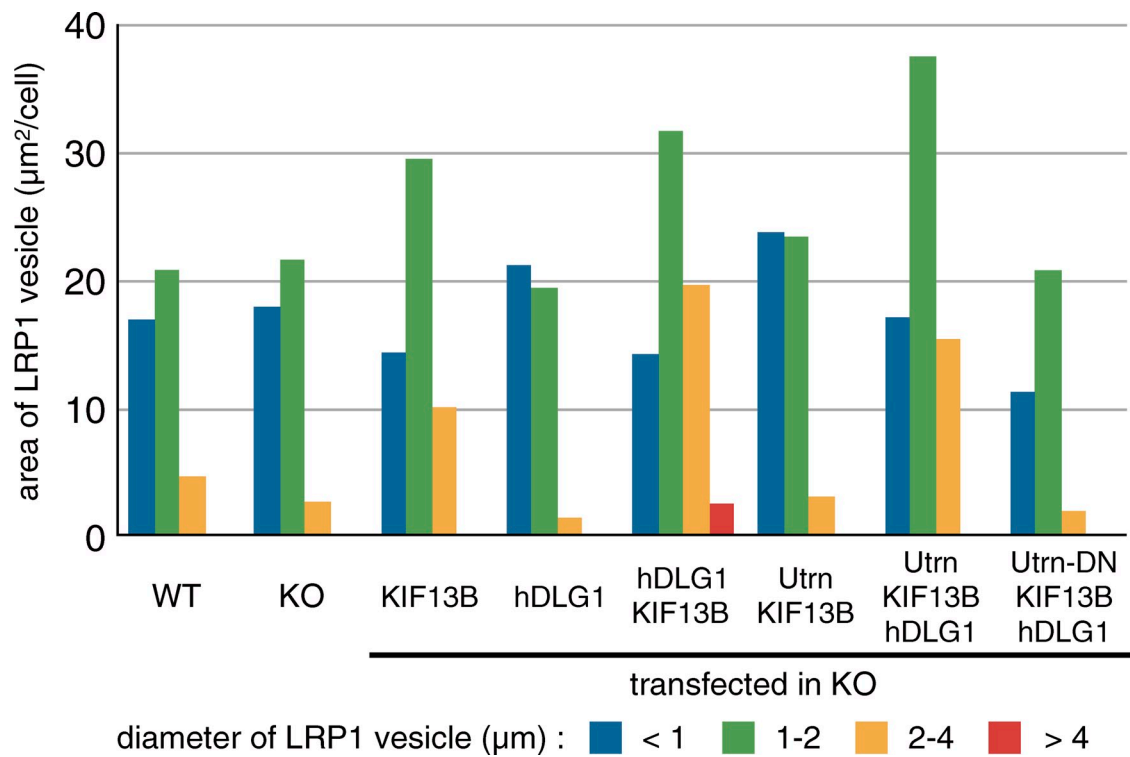


Figure S4. **Quantitative analyses of the size of LRP1-containing vesicles.** Histogram of the size of LRP1-containing vesicles in WT MEFs, KO MEFs, and a series of transfected KO MEFs in Figs. 3, 6, and 7. LRP1-containing vesicles were classified according to their diameters ( $\sim 1$   $\mu\text{m}$ ,  $1\text{--}2$   $\mu\text{m}$ ,  $2\text{--}4$   $\mu\text{m}$ , and  $4$   $\mu\text{m}$ ). Their total areas per cell were shown ( $n = 21\text{--}27$  cells,  $>1,000$  vesicles/transfection condition). "WT" and "KO" correspond to Fig. 3 E. "KIF13B" corresponds to Fig. 3 A. "hDLG1" and "hDLG1 + KIF13B" correspond to Fig. 6, B and C, respectively. "Utrn + KIF13B", "Utrn + KIF13B + hDLG1", and "Utrn-DN + KIF13B + hDLG1" correspond to Fig. 7, H, I, and K, respectively.